



**International Journal of Critical Infrastructures**

ISSN online: 1741-8038 - ISSN print: 1475-3219

<https://www.inderscience.com/ijcis>

---

**Applying artificial rabbit optimisation-LSSVR analysis for HPC's compressive strength estimation**

Jianjian Wang, Zhigang Liu, Guanglei Zhao

**DOI:** [10.1504/IJCIS.2026.10068986](https://doi.org/10.1504/IJCIS.2026.10068986)

**Article History:**

|                   |                   |
|-------------------|-------------------|
| Received:         | 06 September 2024 |
| Last revised:     | 01 December 2024  |
| Accepted:         | 07 December 2024  |
| Published online: | 11 September 2025 |

---

## Applying artificial rabbit optimisation-LSSVR analysis for HPC's compressive strength estimation

---

Jianjian Wang\*, Zhigang Liu and  
Guanglei Zhao

School of Architectural Engineering,  
Henan Vocational University of Science and Technology,  
Zhoukou, Henan, China

Email: wangjjabm@163.com

Email: zhigangliu913@gmail.com

Email: hkzdzgl@sina.com

\*Corresponding author

**Abstract:** High-performance concrete (HPC) functions stronger because it contains more components than ordinary concrete. The compressive strength (CS) of HPC prepared with fly ash (FA) and blast furnace slag (BFS) was assessed using several artificially-based analytics. In this study, the artificial rabbit optimisation (ARO) technique, abbreviated as AROR and AROLS for the radial basis function (RBF) neural network and the least square support vector regression (LSSVR) analysis, accordingly, was employed to identify the optimal values for the parameters that could be adjusted to enhance performance. The CS was used as the predicting objective, and 1,030 experiments and eight input parameters were used to construct the suggested techniques. After that, the outcomes of the enhanced model were compared to those documented in the corpus of current scientific literature. The calculations suggest that combining AROLS with AROR research might be advantageous. The AROLS demonstrated much higher  $R^2$  ( $R^2_{\text{Train}} = 0.9853$  and  $R^2_{\text{Test}} = 0.9912$ ) and lower error metrics when compared to the AROR and previous papers. Finally, the offered technique for computing the CS of HPC increased by BFS and FA may be created using the recommended LSSVR analysis enhanced by ARO.

**Keywords:** high-performance concrete; compressive strength; artificial neural network; least square support vector regression; artificial rabbit optimisation.

**Reference** to this paper should be made as follows: Wang, J., Liu, Z. and Zhao, G. (2025) 'Applying artificial rabbit optimisation-LSSVR analysis for HPC's compressive strength estimation', *Int. J. Critical Infrastructures*, Vol. 21, No. 8, pp.1–28.

**Biographical notes:** Jianjian Wang, who graduated from North China University of Water Resources and Electric Power in 2017, is currently a faculty member at Henan Vocational University of Science and Technology, located in Zhoukou, Henan, 466000, China. His primary research focus is on developing and applying machine-made sand fly ash concrete, aiming to enhance the performance and sustainability of construction materials.

Zhigang Liu is a faculty member at Henan Vocational University of Science and Technology in Zhoukou, Henan, 466000, China. His research interests lie in energy efficiency in green buildings and the corrosion resistance of construction materials. His work focuses on developing innovative evaluation

methods for assessing the energy-saving potential and enhancing the durability of construction materials, contributing to more sustainable and resilient infrastructure. His research plays an important role in promoting green building practices and improving the longevity and safety of construction materials in challenging environments.

Guanglei Zhao graduated from Zhengzhou University of Aeronautics in 2007 with a degree in engineering. He works at Henan Vocational University of Science and Technology in Zhoukou, Henan, China (466000). His primary research interest is machine-made sand fly ash concrete, focusing on its properties, applications, and environmental benefits in the construction industry.

---

## 1 Introduction

High-performance concrete has become a ‘must’ building material in almost all modern construction works because of its strength, durability, and lifespan, which are superior to conventional concrete. The American Concrete Institute, ACI, defines HPC as concrete that consists of very high criteria for various performance parameters, including but not limited to compressive strength, workability, durability, and consistency (Benemaran et al., 2024; Mathew et al., 2024a). Properties make it apt for demanding applications like bridges, high-rise buildings, and structures exposed to severe environmental conditions (Szolomicki and Golasz-Szolomicka, 2019). Durability stands out of all the salient benefits of HPC compared to normal concrete (Abdul Nabi and Kadhim, 2020). Whereas the latter is prone to several problems, such as cracking, corrosion, and shrinkage after a certain period, HPC is made resistant to such breakdowns (Ding et al., 2021; Pandey et al., 2024). This is achieved by adding special additives and optimisation in mix designs to reduce permeability, increase resistance to chemical attack, and improve resistance against freeze-thaw (Pulivarthy, 2024). Improved durability increases the structure’s service life, reducing the frequency of repair and maintenance (Pierre et al., 2024a). This will bring about considerably more savings in a longer period (Bader and Lackner, 2020; Panyaram, 2024).

Increased service life and reduction of maintenance costs are particularly important in infrastructure projects, where any downtime or loss of structural integrity can be critical (Lukutin and Kadhim, 2021a). In this respect, HPC represents a real service life extension compared to conventional concrete, which can often be repaired or even replaced under various environmental stresses (Rincon et al., 2024; Ikwuagwu et al., 2023). These long-term savings against its usually higher initial cost make HPC the cost-effective choice for some high-performance applications (Kadhim and Lukutin, 2021). This, however, is not as easy as making normal concretes (Pierre et al., 2024b). Normal concrete mixes cement, water, and aggregates in standard proportions, typically modified by achievable strength and workability (Nwezeh, 2023; Kadam and Deming, 2024). HPC mixtures allow for additional cementitious materials such as silica fume, fly ash, and GGBFS to improve the concretes’ properties (Alhusseini et al., 2024; Nwabuokei et al., 2023; Thirunagalingam, 2024a). Materials intended for strengthening and reducing the water-cement ratio and improving the resistance of concrete against the action of external aggressive media (Jasper et al., 2024; Mathew et al., 2024b; Usman and Ullah, 2024).

Superplasticisers are the most common chemical admixtures used in producing HPC, which enhance workability without adding extra water (Sucharda et al., 2024; Santoso et al., 2021).

Compressive strength in the performance of HPC is one of its main features (Mudunuri, 2024; Saxena et al., 2023). It is one of the indicative factors in the material's ability to bear a mechanical load and different stresses without failure (Ikwuagwu et al., 2024a; Suraj et al., 2024). Compared with traditional concrete, HPC shows a very high value of CS that ensures superior performance in the most extreme loading conditions (Zhao et al., 2024; Mehta et al., 2023; Tin et al., 2024). The mix design of HPC is fine-tuned to the respective proportions of various materials combined, such that a proper balance between the desired strength and durability characteristics is obtained (Al-Zubaydi and Kadhim, 2023). Advanced models allow a far larger degree of precision for predicting HPC behaviour under varying environmental and load conditions compared to what has been experienced (Banala, 2024; Kadhim and Lukutin, 2019; Thirunagalingam, 2024b). One of the major disadvantages of HPC involves cost and material availability (Abdal et al., 2023; Zanardo, 2024). Indeed, inclusion in HPC of supplementary cementitious materials and chemical admixtures can increase its cost, while the availability of certain ingredients may vary in different regions (Anand et al., 2024; Nanban et al., 2024). While choosing a proper HPC mix design, the required performance should be weighed against local material availability and respective costs (Hadji et al., 2021; Kumar et al., 2024).

Besides, HPC requires more complex quality control and more elaborate varieties of tests than normally used in regular concrete, which is again reflected in its final price (Elaiyaraja and Boinapalli, 2024). Although HPC is superior in its performance, conducting even more detailed and scrupulous testing is necessary to ensure dependability (Lukutin et al., 2022; Maraju, 2024). Mix design in HPC has to be tested for various conditions to realise whether it meets the intended strength, workability, and durability (Lukutin and Kadhim, 2021b). Some test areas involved are compressive strength, shrinkage permeability, and resistance to environmental degradations (Alomayri et al., 2023). Additional tests would be required, considering variable raw materials and environmental conditions in which the mix must be suitable for the intended use. Statistical regression techniques have already played a major role in fine-tuning HPC mix designs (Gupta et al., 2024). These kinds of methods permit an examination of complex relationships between various ingredients and the properties of concrete. Such methods shall enable researchers to optimise mix design for certain performance goals and thereby make such HPC meet a project's technical and economic requirements (Ikwuagwu et al., 2024b; Regin et al., 2021). This will also allow the engineer to statistically model and simulate HPC performance or behaviour under various environmental exposure conditions, such as extreme weather, heavy traffic loads, or aggressive chemical environments (Tiza et al., 2024; Raja et al., 2024).

## **2 Literature review**

Data mining has lately attracted a lot of attention from the academic and industrial areas to handle engineering-related problems (Benemaran, 2023; Esmacili-Falak and Benemaran, 2024a, 2024b). It might be quite advantageous to construct computer

simulations using data mining frameworks where research can be conducted. Professionals have recently utilised a variety of AI-based algorithms to forecast concrete mechanical properties. Additionally, Erdal et al. (2013) predicted the CS of HPC using bagged artificial neural networks (ANN) and gradient-boosted ANN. Regression trees, NNs, support vector machines (SVM), and chi-squared automated interaction detectors were investigated by Chou and Pham (2013) to assess the mechanical characteristics of different construction materials.

Golafshani et al. (2022) proposed a tool that could estimate compressive strength via several data-driven techniques. In this regard, they extended multi-layer neural networks and radial basis function neural network models to the Harris hawks optimisation algorithm on a dataset that included 1,374 concrete mixture proportions, curing age, and values of CS. This hybridised model outperformed all the other models. Of all such variables, the most influencing ones on CS were cement, coarse aggregates, and fine aggregates, while slag, fly ash, and concrete age had less influence.

Prakash et al. (2024) estimated the compressive strength of UHPC through nine hybrid machine-learning models involving different optimisation algorithms. The models developed in this study have used ANN and algorithms such as ALO, GWO, SSA, WOA, DA, PSO, HHO, SMO, and GTO using a dataset of 308 observations. The best model developed for ANN-GTO presented  $R^2 = 0.9629$  and  $RMSE = 0.0518$  in modelling and  $R^2 = 0.9578$  and  $RMSE = 0.0540$  during testing. Therefore, sensitivity and uncertainty analyses prove that the model will serve the purpose appropriately and thus be useful in civil engineering projects. Bian et al. (2024) applied RBF and XGB models to predict and optimise compressive strength in SCC mixtures. For this purpose, supplementary admixtures such as lime powders, fly ash, and silica fume were added to the dataset of experimental samples. NGOA and HGSO are applied to these models to give their four variants: XGBNG, XGBHG, RBFNG and RBFHG. Their XGBNG model gave the best precision, reaching a minimum OBJ value of 0.8062, followed by XGBHG, with an OBJ value of 1.657, RBFNG with an OBJ value of 2.4891, and RBFHG with an OBJ value of 3.9131.

Nguyen and Ly (2024) proposed integrating the GBR with three metaheuristic optimisation algorithms, such as SCSO, GWO\_WOA, and ARO, for the axial compressive capacity prediction of the CFDS-ST columns. Considering the experimental results obtained for 153 data, GBR optimised through the ARO algorithm outperformed eight machine learning models, three design standards, and two empirical equations in prediction. The model optimised a CFDSST column design for maximum ACC, considering the design constraints, which improved the safety and efficiency of CFDSST structures.

Imran et al. (2024) investigated the prediction of compressive strength in high-performance concrete using machine learning to overcome some tedious conventional methods. Using a large database, the models compared in this research effort include GPR, DT, MLR, SVM, and BR. The GPR model showed the best performance, with  $R^2$  at 0.943, RMSE at 4.397, and MAE at 3.230. These were followed by cement, coarse aggregate, sand, and water as the most relevant. GPR gave the best prediction accuracy in the present work; hence, it will be cost-effective and sustainable to estimate the compressive strength of HPC using GPR. Li et al. (2023) proposed a neural network model, RBFNN, for estimating the compressive strength and slump of HPC mixtures to reduce expensive experiments and improve precision. The model training was metaheuristically optimised using HGSO and multiverse optimiser techniques, including

fly ash and superplasticiser, in 181 HPC mixture datasets. Performed identically well, the MVO-based model outperformed it by having a smaller RMSE in a slump and accordingly 3.7 versus 5.3 mm and a higher  $R^2$  in slump flow rates, 98.25% versus 96.86%. Both of these hybrid models predicted the hardness properties of HPC samples (Ramya et al., 2023).

ANNs are the most studied learning methods, according to empirical efforts. ANNs are widely utilised to evaluate several tangible attributes (Lee, 2003; Ji et al., 2006; Yeh, 2007; Amlashi et al., 2023). With these, predictions have been made regarding the CS and slump flow of HPC mixes (Kasperkiewicz et al., 1995; Prasad et al., 2009). In order to assess the CS of HPC, Rajasekaran and Lavanya (2007) utilised a wavelet neural network technique. Piro et al. (2022a) used multi logistic regression (MLR), an ANN, and a full quadratic (FQ) model to forecast the electrical resistivity (ER) and CS of concrete containing ground-granulated blast-furnace slag (GGBS) and steel slag (SS). The ANN predicted the concrete's CS and ER more accurately than MLR and PQ. In a similar work, Piro et al. (2022b) evaluated the CS of concrete, including natural aggregates like steel slag, fine aggregate, and coarse aggregate, using a complete FQ, an M5P tree model, an ANN, a nonlinear regression (NLR), and a linear LR. It is possible to explain further study using various machine learning (ML) techniques. The CS of HPC was estimated using gradient-boosted ANN and bagged ANN (Hir et al., 2023). Chou and Pham's (2013) cluster methods fared well compared to previous experiments. Rafiei et al. contrasted the effectiveness of their newly introduced deep machine with that of SVR and backpropagation NN (Rafiei et al., 2017b). With actual testing data from the UC Irvine ML reservoir, they find that the existing framework is only 98% accurate at most. The density of foamed concrete was calculated using a deep neural network architecture (Nguyen et al., 2019). An optimisation method provided a new solution to the concrete mix design issue (Rafiei et al., 2017a). For the CS of HPC mixes, new prediction work coupled orthogonal least squares (OLS) with genetic programming (GP) techniques.

Atici (2010) created a regression model for predicting concrete strength using non-destructive testing methods and then conducted statistical tests to confirm the model's correctness. Zain and Abd (2009) calculated HPC's durability using multivariate power equations, which is significantly harder to predict than regular concrete due to the intricate interactions between its constituent parts and visible characteristics. The substantial nonlinearity in the interaction between its constituent parts and physical features makes it difficult to develop a mathematical model that can estimate the computing strength of HPC from the provided data.

Chou et al. (2011) suggested a collection of supervised learning models that can predict the advancement of carbon capture and storage (CCS) technology as an example. According to the authors' analytical results, multiple additive regression trees provide better prediction accuracy than other methods. When it came to predicting the elastic modulus of conventional and high-strength concrete. Yan and Shi (2010) discovered that SVM performed better than other models. This implies that SVM can produce predictions of this sort with extremely high accuracy. Along with other ML approaches like SVM, ANN is a dependable tool for forecasting CCS results by generating mapping functions. However, no single model has consistently been shown to estimate CCS findings better.

An extreme gradient boosting (XGBoost) was employed to train an extremely precise ML model. The study provided further a simple and free user interface to support the design of normal- and high-strength BFS and FA concrete. The compressive strength of 1,030 concrete mixes containing cement (C), BFS and FA were collected and analysed. The baseline model tends to overfit, with  $R^2$  values of 0.996 and 0.919 for the training and testing datasets, respectively (Khan and Abbas, 2023). In another paper, the CS of concrete containing BFS and FA was estimated using coupling the ANFIS with improved grey wolf algorithm and dragonfly optimisation algorithm are innovative algorithms that estimate estimated compressive strength for lab results, in mo. This article noted that the ANFISDA hybrid model performs better than ANFISI\_GWO (Hu, 2023).

### 3 Main contribution

Gene expression programming (GEP), adaptive neuro-fuzzy inference system (ANFIS), multivariate adaptive regression splines (MARS), and other research have all used input variables provided to the method for forecasting the target-dependent variables. However, SVR and RBF neural networks may be able to reduce errors and increase model precision throughout the modelling procedure. The study often finds no correlation between LSSVR and RBF and optimisation techniques, even though different models are being attempted to forecast the mechanical properties of concretes (Cheng et al., 2014; Abd and Abd, 2017; Al-Fugara et al., 2022; Zhang et al., 2020; Li et al., 2021; Lyu et al., 2021; Moodi et al., 2022; Regin et al., 2024). ARO was used in this work to identify the essential components of the LSSVR and RBF approaches that may be changed. The CS of HPC was the prediction aim, and 1,030 trials and eight input factors the primary admixture component, mix designs, and curing age were used to evaluate the proposed models. The application of ARO significantly improved prediction accuracy and stability in both the AROR and AROLS. ARO's adaptive mechanism allows for quick convergence on optimal solutions, often requiring fewer iterations than traditional optimisers. ARO enhanced the optimisation process by effectively balancing exploration and exploitation, minimising the risk of local minima, and ensuring that model parameters are optimised to their fullest potential. Finally, the successful implementation of ARO in predicting HPC compressive strength suggests its potential for broader applications in other predictive models for concrete and construction materials. This study contributes to the current literature in several key ways:

- By combining ARO with LSSVR (AROLS), this study demonstrates an improvement in predictive accuracy over both traditional methods and other artificial intelligence-based approaches. The reported  $R^2$  values and minimised error metrics signify the model's precision, which could be crucial for accurate, reliable predictions in HPC research.
- The use of ARO as an optimisation method for fine-tuning model parameters is relatively novel in HPC research. By comparing the performance of ARO-optimised RBF and LSSVR models, this study provides insights into how optimisation techniques can enhance AI-based models' predictive capabilities, laying the groundwork for further exploration of optimisation algorithms in concrete science.

- This research contributes to sustainable construction by focusing on HPC enhanced with FA and BFS, both of which are more environmentally friendly alternatives to conventional concrete materials. The model's ability to predict CS accurately supports the broader adoption of these materials by enabling engineers to optimise concrete mixes for specific structural requirements.
- With a large dataset of 1,030 samples and a rigorous comparative approach, this study provides a substantial dataset for evaluating different machine learning techniques.

## 4 Data properties and considered algorithms

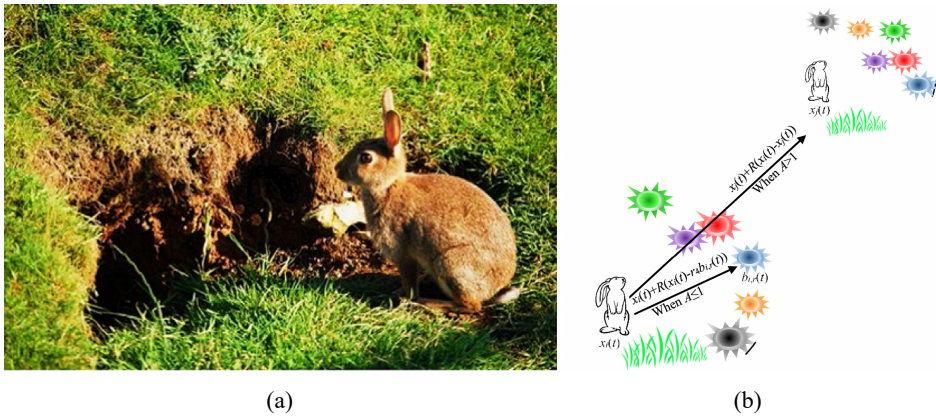
### 4.1 Artificial rabbit optimisation algorithm

In terms of analysis, the actual-world survival strategies of rabbits are represented by an effective optimisation model by the suggested AROA [Figure 1(a)]. This deals with two tactics that are imitated: eating on the detour and unintentionally hiding. Initially, the detour foraging technique is replicated, in which the rabbit is compelled to consume the grass around nearby lairs to conceal its residence from potential adversaries. Second, using the randomised hiding strategy could reduce the chance that an opponent would capture a rabbit. Energy loss may also transpire during the third phase, which might prompt rabbits to adopt an irregular concealment approach in place of their detour feeding tactic (Wang et al., 2022). Every position in the original population is given a random location within the search region, according to equation (1):

$$Rb_i = LB + rand(1, dim) \times [UB - LB] \quad i = 1 : N_{Rb} \quad (1)$$

The above formula indicates each rabbit's location as  $Rb_i$  the lower and upper bounds of the design variables as  $LB$  and  $UB$ , and the overall amount of rabbits in the population as represented by  $N_{Rb}$  and the overall amount of variables under evaluation as  $dim$ .

**Figure 1** (a) A rabbit nest with several burrows (b) Search mechanism based on the energy factor  $A$  (see online version for colours)





#### 4.1.1 Detour forage tactic

According to the AROA's detour foraging technique, each seeking rabbit chooses to participate in the diversion by switching spots with another randomly chosen searching rabbit from the swarm. The following formula illustrates how rabbits use foraging as a diversion:

$$NRb_k(iter+1) = Rb_j(iter) + (Rb_k(iter) - Rb_j(iter)) \times Zm \\ + NDS \times round\left(\frac{1}{2} \times \left(\frac{5}{100} + r_1\right)\right), \quad k, j = 1 : N_{Rb}, j \neq k \quad (2)$$

$$Zm = c \times \left(e - e^{\left(\frac{iter-1}{Iter_{max}}\right)^2}\right) \times \sin(2\pi r_2) \quad (3)$$

$$c(j) = \begin{cases} 1 & \text{if } j = g(\psi) \\ 0 & \text{else} \end{cases}, \quad j = 1 : \text{dim and } \psi = 1 : [r_3, \text{dim}] \quad (4)$$

$$g = randperm(\text{dim}), n_1 N(0, 1) \quad (5)$$

The above formulas state that *iter* specifies the current iteration, *NDS* indicates the regular distribution normal function, and *NRb<sub>k</sub>* and *Rb<sub>k</sub>* denote the new and old locations of the *k*<sup>th</sup> rabbit. Randperm is the name of a randomising transposition function. Three random numbers in the scope [0, 1] are shown by *r*<sub>1</sub>, *r*<sub>2</sub> and *r*<sub>3</sub> and the maximum number of iterations is shown by *Iter<sub>max</sub>*.

#### 4.1.2 Randomised hiding tactic

A rabbit often dig tunnels close to its burrow for shelter while warding off attackers. The equation is provided here from this perspective.

$$b_{k,j}(iter) = Rb_k(iter) \times (1 + H \cdot G) \quad (6)$$

$$k = 1 : N_{Rb} \text{ and } l = 1 : \text{dim} \quad (7)$$

$$H = r_4 \times \frac{Iter_{max} - iter + 1}{Iter_{max}} \quad (8)$$

$$G(j) = \begin{cases} 1 & \text{if } i + k \\ 0 & \text{else} \end{cases}, \quad j = 1 : \text{dim} \quad (9)$$

The *j*<sup>th</sup> tunnel of the *k*<sup>th</sup> bunny is denoted by *b<sub>k,j</sub>*, and *r*<sub>4</sub> seems to be an integer chosen randomly between [0, 1]. *H* represents the concealed value, which progressively reduces from 1 to 1/*Iter<sub>max</sub>* according to the current iteration. This trait suggests that these tunnels were initially built in a bigger rabbit habitat. As the number of repeats rises, this region gets smaller. In order to survive, rabbits must locate a safe place to live. They randomly choose one between the several holes they must hide in to prevent being discovered. This randomised concealment technique may be defined using the algebraic equation as follows:

$$NRB_k(iter+1) = Rb_k(iter) + Zm \times (r_3 \times b_{k,j}(iter) - Rb_k(iter)) \quad k = 1 : N_{Rb} \quad (10)$$

The location of the  $k^{\text{th}}$  rabbit is altered as follows if successful diversion foraging or arbitrary concealment:

$$Rb_k(iter+1) = \begin{cases} Rb_k(iter) & f(Rb_k(iter)) \leq f(NRb_k(iter+1)) \\ NRb_k(iter+1) & f(Rb_k(iter)) > f(NRb_k(iter+1)) \end{cases} \quad (11)$$

#### 4.1.3 Energy decline

Energy is involved in modelling the transition from the discovering state associated with detour foraging to the exploitation stage associated with randomised hiding. The explanation of the factor of energy (AF) [Figure 1(b)] is as follows:

$$AF(iter) = 4 \times in \frac{1}{r} \times \left( 1 - \frac{iter}{Iter_{\max}} \right) \quad (12)$$

#### 4.2 RBF network

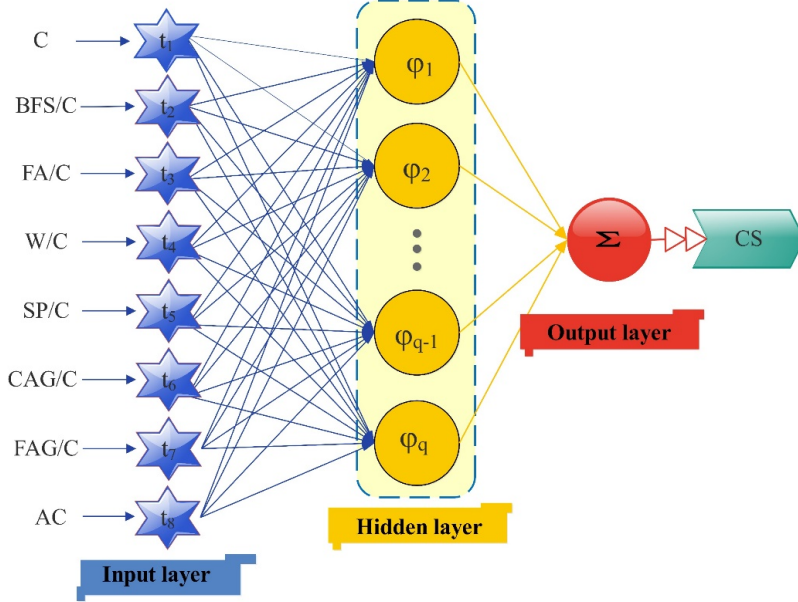
Scholars use RBF, a calculating solution, in simulations (Broomhead and Lowe, 1988; Pierini et al., 2012). Three layers make up an RBFNN. The input layer contains a dataset's input variables. A nonlinear feature that uses the RBF to reduce the dimensionality of the model receives the variables from the input layer. Technique formulation (Buhmann, 2000) states that RBF is a true-valued conductor connected with the present location and space from the source. The linear result layer combines the nonlinear projection results from the hidden layer, which are then applied to the linear regressor. Consequently, the regressor weights are determined using the linear least-squares method. Accordingly, the midline of the RBF and the input are indicated by the variables  $x$  and  $c$  in the method function  $\phi(x, c)$ . The  $\phi$  varies according to the radial space of the input from the midline,  $r = \|x - c\|$ . By summing the linear weights of the neurons in the hidden portions, one may calculate the result of a problem using equation (13).

$$f(x) = \sum_{i=1}^N c_i \phi(\|x - x_i\|) \quad (i = 1, 2, \dots, N) \quad (13)$$

The determination of the size and the appropriate number of concealed layers provide two difficult aspects of *RBF*, nevertheless. In relation to one another, the hidden layer should provide the constant spread and neuronal values. The most useful *RBF* is conducted by perfectly combining the previously described elements. Trial and error led to the discovery of these two values in earlier studies (Kisi and Cigizoglu, 2007; Kisi, 2008; Zaji and Bonakdari, 2014). The most precise *RBF* network is obtained in this research by using the combined AROA-RBF design. The RBF structure, also known as AROR, is found by using the ARO approach, which yields the number and spread value of hidden neurons (Figure 2). The purpose of the RBF neural network in this study is to model the nonlinear relationships between input parameters and the compressive strength

of HPC. RBF networks are particularly effective for capturing complex patterns in data because they use radial basis functions that respond to different regions of the input space, enabling precise predictions even when interactions between variables are intricate.

**Figure 2** RBF neural network schematic (see online version for colours)



#### 4.3 Least square support vector regression analysis

The SVR's capacity to precisely forecast the accumulation rate is constrained by its computational complexity. Moreover, it is important to remember that this method may result in significant overhead processing. Adopting the LSSVR model is one suggested approach for traditional SVR models to address this issue. Unlike quadratic formulas, the current technique was designed to handle both nonlinear and linear equations. As a significant extension of SVR, the LSSVR model has remarkable abilities for both fitting and generalisation. By employing the square error as the objective function, it is feasible to obtain a significant decrease in computing load and a gain in computational efficiency. In several disciplines, the least squares technique has been the standard data management and analysis approach. The formula for the multiple nonlinear regression model is  $f(x_i) = \omega^T \phi(x_i) + b + \varepsilon$ , wherein the variable vector  $\omega \in R^N$  is determined using the *LSSVR*.

$$g_{LSSVR} = \frac{1}{2} \omega^T \cdot \omega + C \sum_{i=1}^N (y_i - \omega^T \cdot \phi(x_i) - b)^2 \quad (14)$$

$$s.t. \ y_i = \omega^T \cdot \phi(x_i) + b + \xi_i \quad (i = 1, 2, \dots, N)$$

The kernel function  $\phi(\cdot)$  was used to map the input space to a higher-dimensional region. In cases when the noise loss has a Gaussian distribution, the *LSSVR* machine can produce forecast results that exactly meet the specifications. The linear regression model's decision function is  $f(x) = \omega^T \cdot x + b$ . The parameters  $b \in R$ ,  $\omega = (\omega_1, \dots, \omega_L) \in R^L$ , and  $x_i \in R^L$  indicate the structure of the regression model. Using the linear regression model and the kernel function  $K(\cdot, \cdot)$ , the kernel approach generates the kernel regression paradigm *LSSVR*.

$f(x_i) = \omega^T \cdot \phi(x_i) + b$  is the nonlinear decision function of the *LSSVR*.  $K(x_i, x_j) = (\phi(x_i) \cdot \phi(x_j))$ ,  $\phi: R^L \rightarrow H$ , where  $H$  denotes a Hilbert area,  $(\phi(x_i) \cdot \phi(x_j))$  the area  $H$ 's inner product, and  $T$  denotes the transpose of the vector. The *LSSVR* model is a robust predictive tool designed to minimise errors in estimating compressive strength. Focusing on reducing squared errors and achieving a balance between accuracy and generalisation, *LSSVR* can handle high-dimensional data and noisy datasets, which is essential for reliable CS predictions across varied HPC compositions. It is evident from the preceding derivation that the *LSSVR* framework's regression outcomes are directly influenced by the kernel function width ( $g$ ) and the penalty factor ( $c$ ). As such, while using it, it is crucial to carefully select the appropriate values for  $g$  and  $c$ . The current study makes use of AROA approaches to keep the model true to the proper values of  $c$  and  $g$ .

#### 4.4 Dataset

This research evaluated  $H$  samples utilized in published articles (Yeh, 1998a, 1998b, 1999, 2003, 2006) and was taken from the UC Irvine repository. The study's findings are included in the extra sources section of this paper. Normal OPC was used to produce every sample, and it was usually treated thereafter. Presently available literature on HPC testing makes samples of different sizes and shapes. Inputs and outputs are as follows:

Inputs:

- the content of cement ( $C$ )
- The rate of BFS to cement ( $BFS/D$ )
- The rate of FA to cement ( $FA/C$ )
- The water-to-cement rate ( $W/C$ )
- The superplasticiser to cement rate ( $SP/C$ )
- The coarse aggregate to cement rate ( $CAG/C$ )
- The fine aggregate to cement rate ( $FAG/C$ )
- The HPC age ( $AC$ )

Output.

#### 4.4.1 CS of HPC

For the training and testing datasets, the distribution plots of these components are shown in Figure 3, while Table 1 shows the ranges of these database entries. The data collection, containing 1,030 items, was split into two sub-sets by guidelines in earlier research: the training stage contained 70% (721) of the dataset, while the testing stage included 30% (309) of the data (Khorsheed and Al-Thubaity, 2013; Leema et al., 2016). The base set was uniformly distributed, so these portions could be chosen randomly. There was no substantial cross-correlation in the 8D input region, indicating that the selection of these input variables was appropriate based on statistical analysis (Yeh, 1998a, 1998b, 1999, 2003, 2006).

**Table 1** Statistical indices are important for the objective and inputs

| Data  | Index              | Output      | Inputs                    |               |                |                 |                 |                 |              |                |
|-------|--------------------|-------------|---------------------------|---------------|----------------|-----------------|-----------------|-----------------|--------------|----------------|
|       |                    | CS<br>(MPa) | C<br>(kg/m <sup>3</sup> ) | $\frac{W}{C}$ | $\frac{FA}{C}$ | $\frac{BFS}{C}$ | $\frac{CAG}{C}$ | $\frac{FAG}{C}$ | AC<br>(days) | $\frac{SP}{C}$ |
| Train | Minimum            | 2.332       | 102                       | 0.267         | 0.0            | 0.0             | 1.552           | 1.226           | 3.0          | 0.0            |
|       | Maximum            | 82.599      | 540                       | 1.882         | 1              | 1.504           | 8.696           | 9.235           | 365.000      | 0.069          |
|       | Standard deviation | 17.718      | 101.84                    | 0.298         | 0.306          | 0.446           | 1.549           | 1.323           | 67.717       | 0.02           |
|       | Skewness           | 0.304       | 0.511                     | 1.163         | 0.989          | 1.467           | 0.596           | 1.194           | 2.993        | 0.245          |
|       | Kurtosis           | -0.549      | -0.692                    | 2.104         | -0.269         | 1.284           | -0.127          | 2.572           | 10.189       | -1.243         |
| Test  | Minimum            | 6.267       | 132                       | 0.2           | 0.0            | 0.0             | 1.716           | 1.135           | 1.0          | 0.0            |
|       | Maximum            | 74.987      | 540                       | 1.694         | 1.430          | 1.584           | 7.148           | 5.993           | 360          | 0.125          |
|       | Standard deviation | 13.44       | 110.075                   | 0.341         | 0.418          | 0.513           | 1.632           | 1.405           | 50.155       | 0.031          |
|       | Skewness           | 0.499       | 0.533                     | 0.554         | 1.043          | 1.036           | 0.580           | 0.556           | 4.229        | 0.873          |
|       | Kurtosis           | 0.214       | -0.228                    | -1.068        | -0.307         | -0.314          | -1.237          | -0.956          | 20.129       | 0.190          |

Scholars used the Pearson correlation coefficient ( $P_{CC}$ ) [equation (15)].

$$\sigma_{y,z} = \frac{\mu(y, z)}{\delta_y \delta_z} \quad (15)$$

The covariance among  $y$  and  $z$ , as well as the normal deviations of  $y$  and  $z$ , are shown by the values of  $\mu(y, z)$ ,  $\delta_y$  and  $\delta_z$  in equation (1). Figure 4 displays the  $P_{CC}$  values between the input and output parameters. When significant positive or negative  $P_{CC}$  impacts are present, and it may indicate poor methodology if the research cannot describe how these effects have impacted the findings. Since some  $P_{CC}$  values were less than 0.531; it is clear that these  $P_{CC}$  values are most likely not the primary source of the multicollinearity issues. A large number of factors have a considerable impact on each other (more than 0.641). Among  $CAG/C$  and  $FAG/C$ , there is the largest  $P_{CC}$  (0.942). Higher negative correlations are also available, which can make forecasting more challenging.  $C$  and  $CAG/C$  had the strongest negative correlations, with a difference of -0.923.

**Figure 3** The distribution of the variables (see online version for colours)

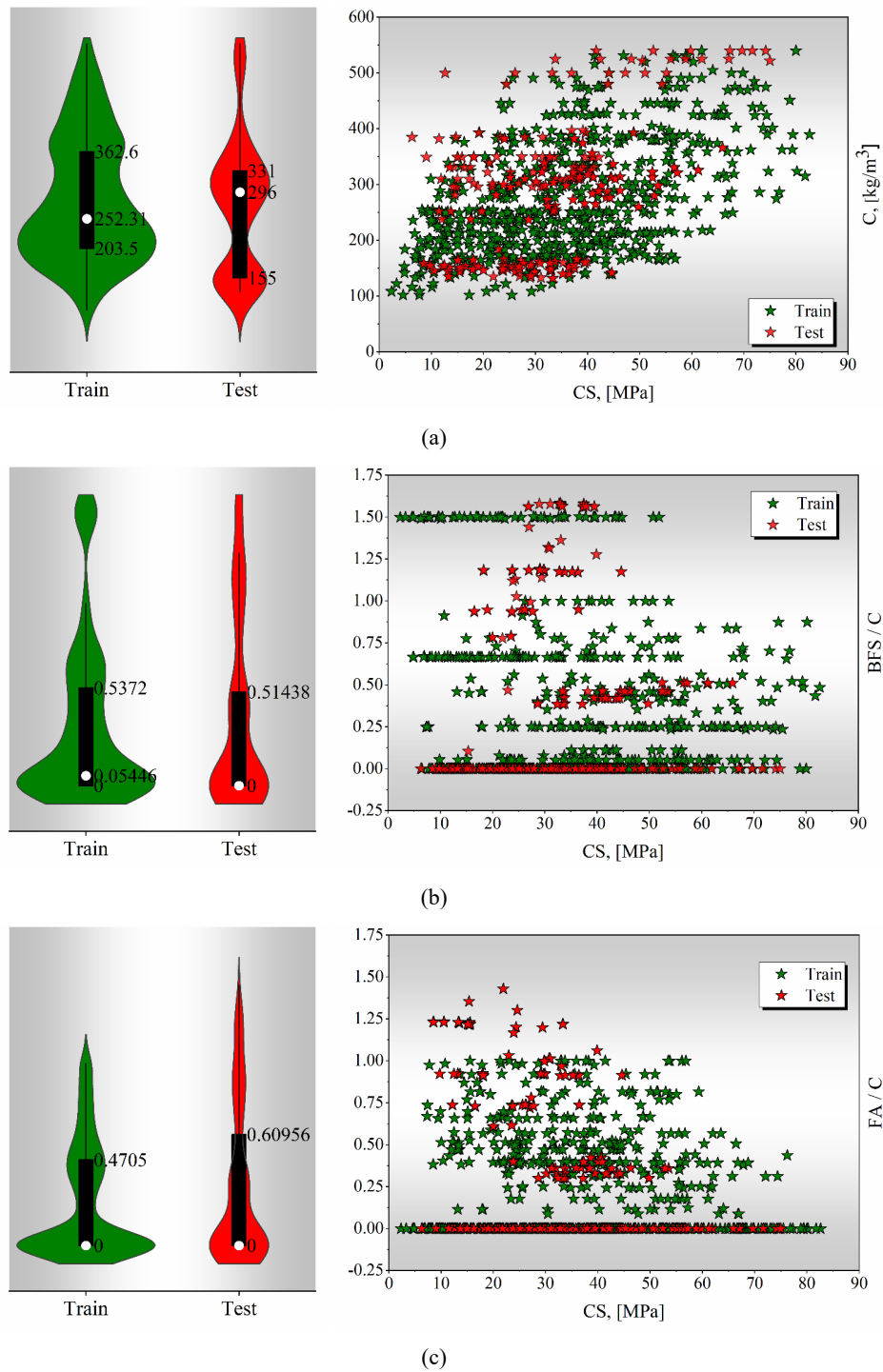
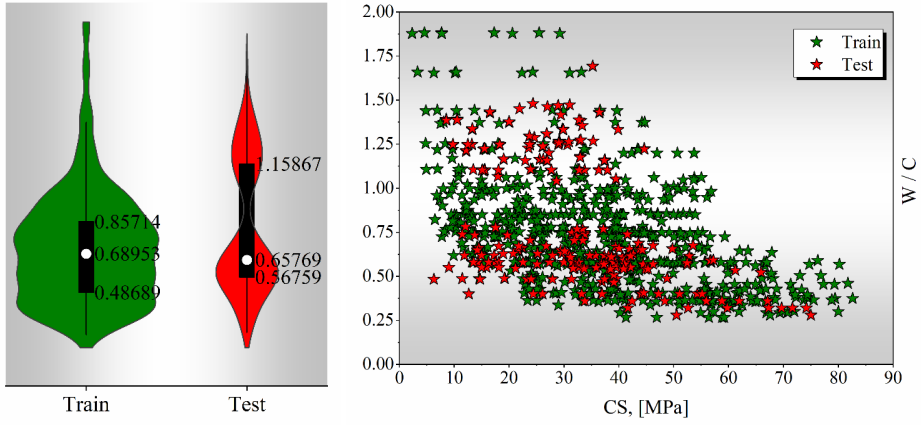
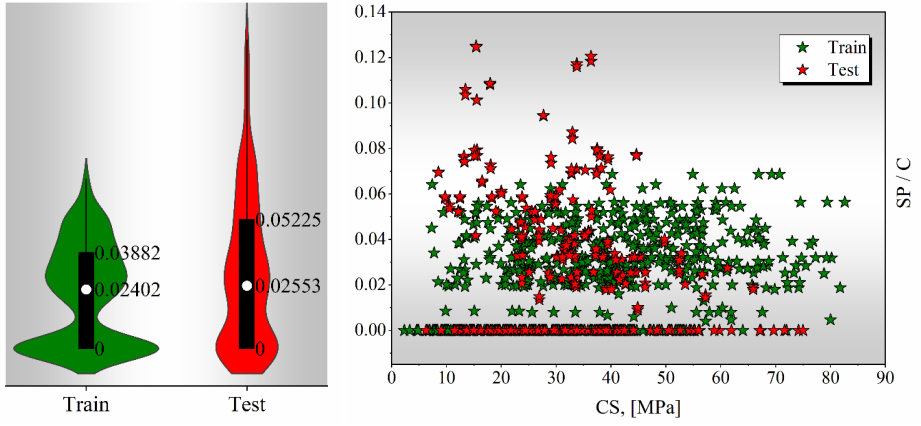


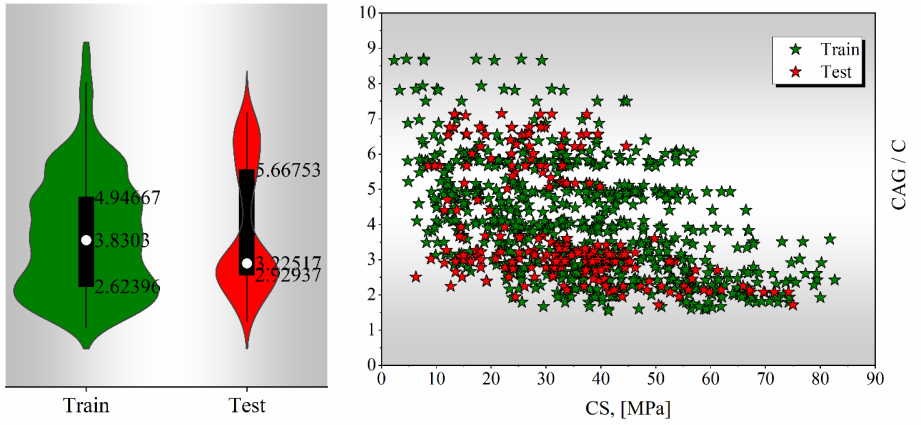
**Figure 3** The distribution of the variables (continued) (see online version for colours)



(d)

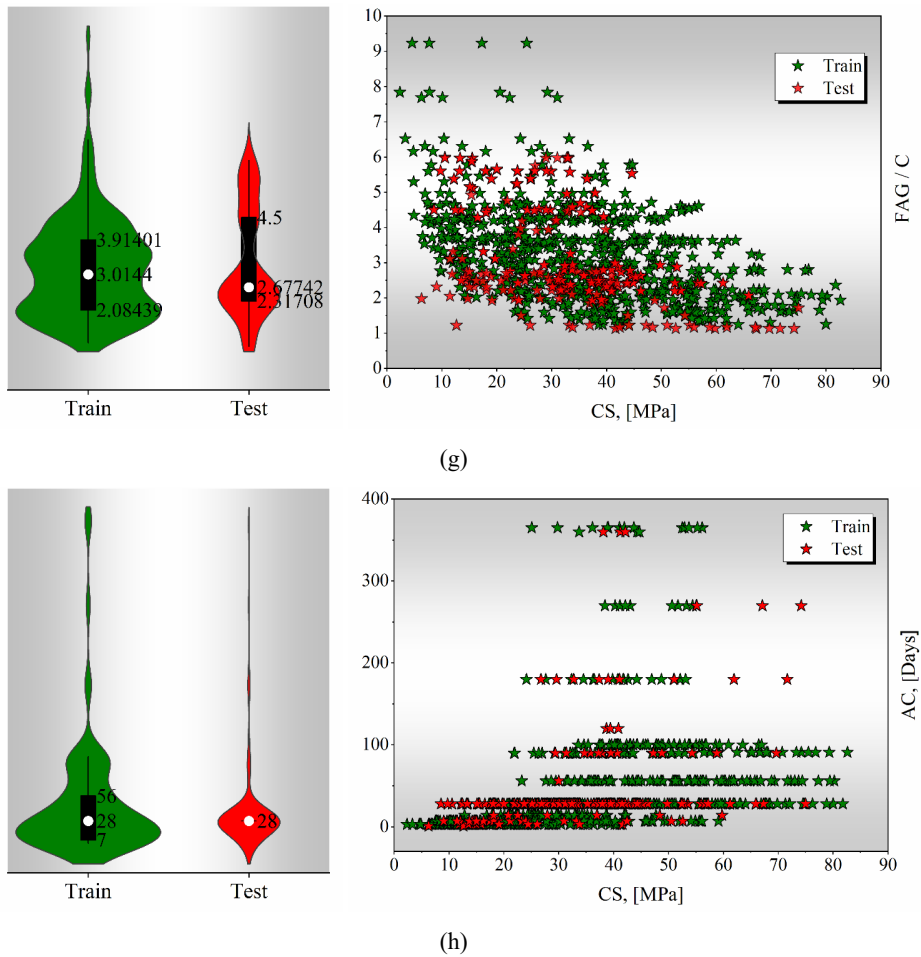


(e)



(f)

**Figure 3** The distribution of the variables (continued) (see online version for colours)





#### 4.5 Evaluation metrics

Six performance measures were used to evaluate the hybrid models. For this purpose, precise measurements [equations (16) to (21)] were made for the coefficient of determination ( $R^2$ ), one extra index ( $A_{20-Index}$ ), relative absolute error ( $RAE$ ), mean absolute error ( $MAE$ ), root relative square error ( $RRSE$ ), and root mean square error ( $RMSE$ ).

$$R^2 = \left( \frac{\sum_{d=1}^D (m_d - \bar{m})(z_d - \bar{z})}{\sqrt{\left[ \sum_{d=1}^D (m_d - \bar{m})^2 \right] \left[ \sum_{d=1}^D (z_d - \bar{z})^2 \right]}} \right)^2 \quad (16)$$

$$RMSE = \sqrt{\frac{1}{D} \sum_{d=1}^D (z_d - m_d)^2} \quad (17)$$

$$MAE = \frac{1}{D} \sum_{d=1}^D |z_d - m_d| \quad (18)$$

$$A_{20-Index} = \frac{d_{20}}{D} \quad (19)$$

$$RRSE = \sqrt{\frac{\sum_{d=1}^D (m_d - z_d)^2}{\sum_{d=1}^D (m_d - \bar{m})^2}} \quad (20)$$

$$RAE = \frac{\sum_{d=1}^D |m_d - z_d|}{\sum_{d=1}^D |m_d - \bar{m}|} \quad (21)$$

where

$m_d$  and  $\bar{m}$  the records and their mean

$z_d$  and  $\bar{z}$  the simulated and their mean

$D$  the dataset's total number

$d_{20}$  the samples' number has a record-per-simulated-individual rate between 0.80 and 1.20.

## 5 Findings and explanation

### 5.1 Discussions

To forecast the CS of the HPC enhanced by BFS and FA, this study shows the results of the ARO-based models (AROP with RBF named AROR and ARO with SLSVR called AROLS). As previously mentioned, the performance of LSSVR and RBF is dependent on the proper proportioning of the constituent elements. The values of the HPC CS observed

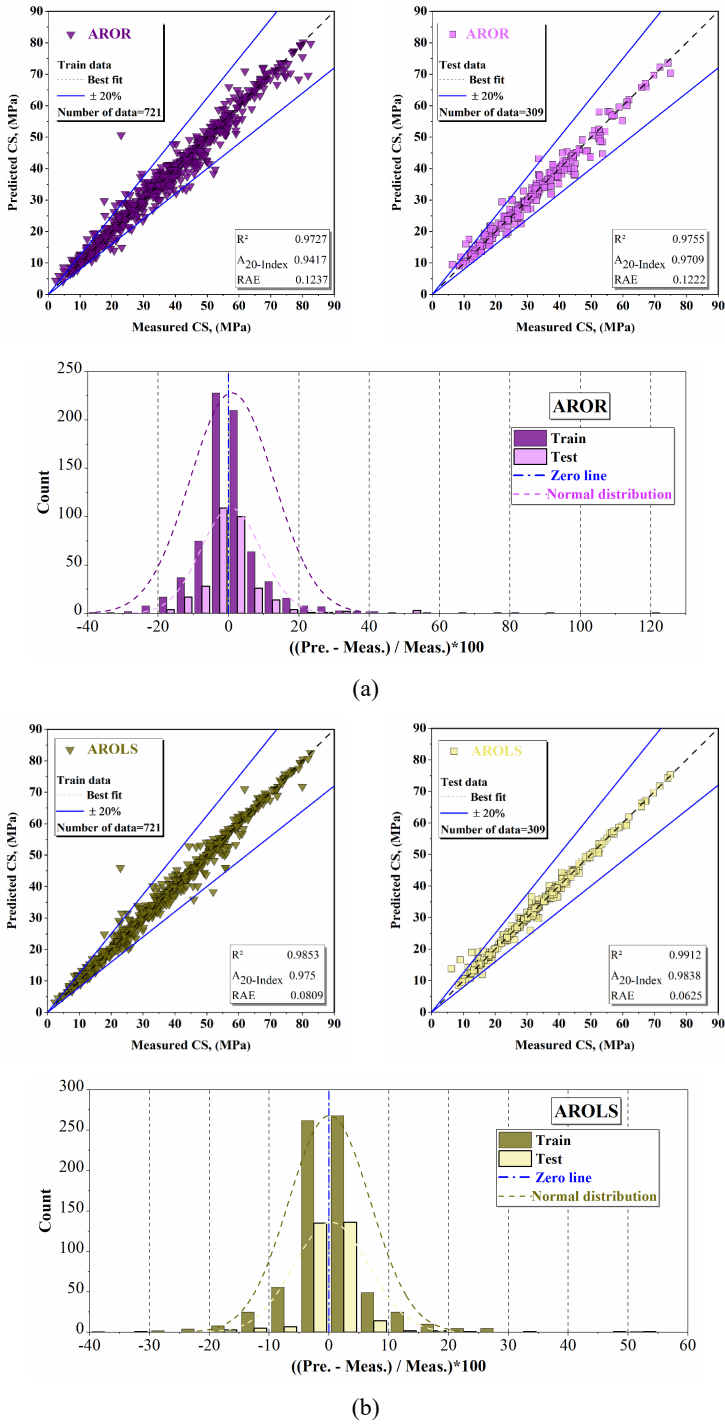
and computed for the AROR and AROLS structures developed throughout the training and testing phases are displayed in Figure 5. Additionally, a normal distribution of curves was used to display the proportion of error in the carbon dioxide (CS) concentration. The central point of the distribution served as a representation of the zero-error percentage line.  $R^2$ ,  $RMSE$ ,  $MAE$ ,  $RAE$ ,  $RRSE$ , and  $A_{20-Index}$  values were used to assess the utility of the AROR and AROLS (Table 2). There is a lot of promise for producing precise estimations of HPC's CS using both AROLS and AROR.

**Table 2** Offered frameworks' performance

| Phase | Metric         | Comparison   |              |                       |                          |                      |                      |                   |                   |
|-------|----------------|--------------|--------------|-----------------------|--------------------------|----------------------|----------------------|-------------------|-------------------|
|       |                | This article | This article | Mousavi et al. (2012) | Gandomi and Alavi (2012) | Chou and Pham (2013) | Nguyen et al. (2021) | Dao et al. (2020) | Lee et al. (2023) |
|       |                | AROR         | AROS         | GEP                   | MGGP                     | ANN                  | SEM                  | GPR               | XGB (all data)    |
| Train | $R^2$          | 0.9727       | 0.9853       | 0.8224                | 0.7885                   | —                    | 0.84                 | 0.888             | 0.944             |
|       | $MAE$          | 1.7949       | 1.1736       | 5.202                 | 5.56                     | —                    | 4.91                 | 3.996             | 2.592             |
|       | $RMSE$         | 2.9374       | 2.1523       | —                     | 7.36                     | —                    | 6.3                  | 5.59              | 3.878             |
|       | $RAE$          | 0.1237       | 0.0809       | —                     | —                        | —                    | —                    | —                 | —                 |
|       | $RRSE$         | 0.1658       | 0.1215       | —                     | —                        | —                    | —                    | —                 | —                 |
|       | $A_{20-Index}$ | 0.9417       | 0.975        | —                     | —                        | —                    | 0.68                 | —                 | —                 |
| Test  | $R^2$          | 0.9755       | 0.9912       | 0.8354                | 0.8046                   | 0.8649               | 0.8567               | 0.888             | —                 |
|       | $MAE$          | 1.2931       | 0.6615       | 5.19                  | 5.48                     | 4.421                | 4.482                | 3.913             | —                 |
|       | $RMSE$         | 2.117        | 1.2684       | —                     | 7.31                     | 6.329                | 5.968                | 5.597             | —                 |
|       | $RAE$          | 0.1222       | 0.0625       | —                     | —                        | —                    | —                    | —                 | —                 |
|       | $RRSE$         | 0.1575       | 0.0944       | —                     | —                        | —                    | —                    | —                 | —                 |
|       | $A_{20-Index}$ | 0.9709       | 0.9838       | —                     | —                        | —                    | 0.752                | —                 | —                 |

The findings of this inquiry were also impartially contrasted with those of other studies that have been released. With  $R^2$  values of 0.9853 and 0.9912 for AROLS and 0.9727 and 0.9755 for the train and test phases of AROR, the combined AROR and AROLS approaches performed rather well in terms of estimation. Choosing the best course of action requires carefully examining and assessing the signals produced. Throughout the train process, the AROLS's  $RMSE$  value decreased relative to the AROR, moving from 2.9374 MPa to 2.1523 MPa. Within the test section, calculations showed a moderate drop from 2.117 MPa to 1.2684 MPa. With  $MAE_{Train} = 1.1736$  MPa and  $MAE_{Test} = 0.6615$  MPa, the  $MAE$  metric also produced similar findings with  $RMSE$ , indicating that the AROLS showed improved capability for CS evaluation. Compared to the AROR, which had  $MAE_{Train} = 1.7949$  MPa and  $MAE_{Test} = 1.2931$  MPa, these values were smaller. A 3% rise in the training segment and a 1.5% rise in the testing part for AROLS were found for the  $A_{20-Index}$  signal, indicating similar results.

**Figure 5** The outcomes of the systems based on ARO, (a) AROR (b) AROLS (see online version for colours)



Before creating the estimations, several approaches were compared and evaluated, including GEP (Mousavi et al., 2012), the semi-empirical method (SEM) (Nguyen et al., 2021), Gaussian process regression (GPR) (Dao et al., 2020), ANN (Chou and Pham, 2013), multi-gene genetic programming (MGGP) (Gandomi and Alavi, 2012), and extreme gradient boosting (XGB) (Lee et al., 2023). With reference to Table 2, it is evident that the proposed AROLS outperformed those found in the literature.  $RMSE$  of 6.3 MPa vs. 2.1523 MPa,  $MAE$  of 4.91 MPa vs. 1.1736 MPa,  $A_{20-Index}$  of 0.68 vs. 0.975, and  $R^2$  of 0.84 vs. 0.9853 indicate that SEM underperformed compared to AROLS (Nguyen et al., 2021). In comparison to AROS, GEP showed a much higher  $MAE$  and a significantly smaller  $R^2$  (at 0.8224 and 5.202 MPa, respectively) (Mousavi et al., 2012). Though it eventually fell short, the most current technique, XGB, came dangerously close to surpassing AROLS (Lee et al., 2023). Other techniques, like MGGP (Gandomi and Alavi, 2012) and ANNs (Chou and Pham, 2013), performed badly when compared to AROLS (0.9853), with  $R^2$  values of 0.8046 and 0.8469, accordingly. In terms of  $R^2$ ,  $RMSE$  and  $MAE$ , the AROS also fared better than the GPR (Dao et al., 2020). Descriptions, arguments, and comparisons all point to the *AROLS* as the best model to use in real-world applications when attempting to estimate the improved computational capacity of HPCs via the employment of FA and BFS.

The application of ARO significantly improved prediction accuracy and stability in both the AROR and AROLS. The study reports  $R^2$  values of 0.9853 (training) and 0.9912 (testing) for AROLS, demonstrating ARO's effectiveness in reducing errors and enhancing model performance in the context of complex, nonlinear relationships. ARO's adaptive mechanism allows for quick convergence on optimal solutions, often requiring fewer iterations than traditional optimisers. ARO enhanced the optimisation process by effectively balancing exploration and exploitation, minimising the risk of local minima, and ensuring that model parameters are optimised to their fullest potential. Finally, the successful implementation of ARO in predicting HPC compressive strength suggests its potential for broader applications in other predictive models for concrete and construction materials.

Figure 5(a) presents the scatter plot of the AROR model, and Figure 5(b) presents the scatter plot of the AROLS model. These plots demonstrate the accuracy of the models, as indicated by data points clustered near the best-fit line, which corresponds to an  $R^2$  value of 1, representing optimal conditions. In the training phase of the AROR model, the data points are widely scattered but mostly close to the best-fit line. This scatter reduces during the testing phase, indicating a slight improvement in model performance. The error line in the AROR model's performance plot further highlights this improvement, with a high count of training and testing datasets near the zero error line, indicating the model's accuracy. In contrast, the AROLS model performs better than the AROR model. The scatter plot of the AROLS model in Figure 5(b) shows a strong connection between the datasets and the best-fit line throughout the training and testing stages. The precision and dependability of the AROLS are demonstrated by the error plot, which displays that most datasets fall between  $-10\%$  and  $+10\%$ .

## 5.2 Limitations of the study

Despite the promising results obtained in this study, several limitations should be acknowledged:

- The controlled experiments may not fully replicate the variability and conditions found in real-world construction environments. Factors such as environmental conditions, material quality, and human error can impact the CS of HPC in practice, which were not accounted for in this study.
- The study focuses on the CS of HPC at specific points in time. It does not consider the long-term performance or durability of HPC, which are critical factors in construction applications. Future research should investigate how these models predict long-term strength and performance under various environmental conditions.
- The models assume that the input parameters and the resulting HPC are homogenous. In practice, variations in mixing, curing, and material properties can lead to heterogeneous characteristics in the concrete, potentially affecting the accuracy of the predictions.
- The reliance on AI-based predictions for critical infrastructure components necessitates a rigorous validation process to ensure safety and reliability. Overreliance on model predictions without thorough validation could pose ethical and safety risks in construction projects.

### 5.3 *Future studies suggestions*

- Investigate the long-term performance and durability of HPC predicted by the AROLS and AROR models. This includes studying the effects of environmental conditions, aging, and other factors that may influence the CS and overall performance of HPC over extended periods.
- Combining ARO with other advanced optimisation techniques, such as genetic algorithms or particle swarm optimisation, may enhance model performance. Comparative studies could identify the most effective combinations for predicting HPC properties.
- Conduct real-world trials to validate the predictive capabilities of the AROLS and AROR models. Collaborations with construction projects can provide practical insights and help refine the models based on real-world data and conditions.
- Extend the study's scope to encompass multifactorial investigation of other HPC mechanical parameters, such as durability metrics, tensile strength, and flexural strength. Understanding the interplay between different properties can lead to more comprehensive predictive models.
- Future studies could integrate sustainability metrics, such as carbon footprint and energy consumption, into the predictive models. This approach aligns with the growing emphasis on sustainable construction practices and can help optimise performance and environmental impact.

The ARO-enhanced LSSVR model provides a reliable method for predicting HPC compressive strength, improving project planning and quality control by allowing precise forecasting of concrete performance before casting. This accuracy supports data-driven decision making, enabling engineers to select cost-effective and sustainable materials, reducing trial-and-error, and optimising resource allocation. Furthermore, the model aids

in risk mitigation, ensuring structures meet safety standards, particularly in projects with high durability requirements. The integration of ARO with LSSVR introduces an effective optimisation approach in concrete science, enhancing the theoretical framework for predictive modelling in complex systems like HPC. This work advances sustainable engineering theory by showing that eco-friendly materials can perform well, offering empirical support for green engineering practices. Additionally, the study provides a benchmark for accuracy in HPC research, guiding future advancements in machine learning applications within material science and civil engineering.

## 6 Conclusions

Developing a method for thoroughly evaluating forecast methods to estimate the CS of HPC was the primary goal of this study. It attempted to develop techniques that could use the LSSVR analysis and RBF neural network to predict the features of HPC both before and after hardening. The ARO, also known as AROLS and abbreviated AROR, were used in this work to determine whether essential elements of the RBF and LSSVR techniques may be changed. The following are the primary findings:

- With  $R^2$  values of 0.9853 and 0.9912 for AROLS and 0.9727 and 0.9755 for the train and test parts of AROR, respectively, the merged AROR and AROLS techniques fared rather well in terms of estimate.
- Throughout the train process, the AROLS's RMSE value decreased relative to the AROR, moving from 2.9374 MPa to 2.1523 MPa. The test segment computations show a modest pressure drop from 2.117 MPa to 1.2684 MPa. Additionally, the RMSE and the RAE, RRSE and MAE metrics yielded similar findings, indicating that the AROLS shown better abilities for CS assessment. Comparable outcomes were seen for the  $A_{20-Index}$  signal, demonstrating an increase for AROLS of 1.5% during testing and 3% during training.
- In terms of comparative findings, it was evident that AROLS outperformed research when stated values  $R^2$ , RMSE,  $A_{20-Index}$ , and MAE indices were taken into account.
- Descriptions, arguments, and comparisons all point to the AROLS as the best model to use in real-world applications when attempting to estimate the improved computational capacity of HPCs via the employment of FA and BFS.

## Authorship contribution statement

*Jianjian Wang*: Writing-original draft preparation, conceptualisation, supervision, project administration. All individuals who meet the criteria for authorship are recognised as authors. Each author attests to their significant contribution to the work, assuming public responsibility for its content, including participation in the manuscript's conceptualisation, design, analysis, writing, or revision.

## References

- Abd, A.M. and Abd, S.M. (2017) 'Modelling the strength of lightweight foamed concrete using support vector machine (SVM)', *Case Studies in Construction Materials*, Vol. 6, No. 1, pp.8–15.
- Abdal, S., Mansour, W., Agwa, I., Nasr, M., Abadel, A., Özkılıç, Y.O. and Akeed, M.H. (2023) 'Application of ultra-high-performance concrete in bridge engineering: current status, limitations, challenges, and future prospects', *Buildings*, Vol. 13, No. 1, p.185.
- Abdul Nabi, R.A. and Kadhim, K.H. (2020) 'Solar PV system for water pumping incorporating an MPPT based bat optimization circuits and systems', *Journal of Advanced Research in Dynamical and Control Systems*, Vol. 12, No. 1, pp.786–794, Special Issue.
- Al-Fugara, A., Ahmadiou, M., Al-Shabeeb, A.R., AlAyyash, S., Al-Amoush, H. and Al-Adamat, R. (2022) 'Spatial mapping of groundwater springs potentiality using grid search-based and genetic algorithm-based support vector regression', *Geocarto International*, Vol. 37, No. 1, pp.284–303.
- Alhusseini, A., Kateeb, R. and Thallaj, N. (2024) 'Chemical composition and ursolic acid quantification in *Plumeria rubra* along the Syrian coast', *FMDb Transactions on Sustainable Applied Sciences*, Vol. 1, No. 1, pp.1–9.
- Alomayri, T., Amir, M.T., Ali, B., Raza, S.S. and Hamad, M. (2023) 'Mechanical, tidal erosion and drying shrinkage behaviour of high performance seawater concrete incorporating the high volume of GGBS and polypropylene fibre', *Journal of Building Engineering*, Vol. 76, No. 10, p.107377.
- Al-Zubaydi, N.A.H. and Kadhim, K.H. (2023) 'Performance of intelligent wind turbine pitch control through PI, PID, and LQR and hybrid of PI and LQR controllers', *International Journal of Intelligent Systems and Applications in Engineering*, Vol. 11, No. 10s, pp.923–941.
- Amlashi, A.T., Golafshani, E.M., Ebrahimi, S.A. and Behnood, A. (2023) 'Estimation of the compressive strength of green concretes containing rice husk ash: a comparison of different machine learning approaches', *European Journal of Environmental and Civil Engineering*, Vol. 27, No. 2, pp.961–983.
- Anand, P.P., Jayanth, G., Rao, K.S., Deepika, P., Faisal, M. and Mokdad, M. (2024) 'Utilising hybrid machine learning to identify anomalous multivariate time-series in geotechnical engineering', *AVE Trends in Intelligent Computing Systems*, Vol. 1, No. 1, pp.32–41.
- Atici, U. (2010) 'Prediction of the strength of mineral-addition concrete using regression analysis', *Magazine of Concrete Research*, Vol. 62, No. 8, pp.585–592.
- Bader, T. and Lackner, R. (2020) 'Acrylic surface treatment applied to architectural high-performance concrete (HPC): identification of potential pitfalls on the way to long-lasting protection', *Construction and Building Materials*, Vol. 237, No. 3, p.117415.
- Banala, S. (2024) 'Enhancing system stability with advanced techniques in site reliability engineering', *AVE Trends in Intelligent Computing Systems*, Vol. 1, No. 2, pp.66–76.
- Benemaran, R.S. (2023) 'Application of extreme gradient boosting method for evaluating the properties of episodic failure of borehole breakout', *Geoenergy Science and Engineering*, Vol. 226, p.211837.
- Benemaran, R.S., Esmacili-Falak, M. and Kordlar, M.S. (2024) 'Improvement of recycled aggregate concrete using glass fiber and silica fume', *Multiscale and Multidisciplinary Modeling, Experiments and Design*, Vol. 7, No. 3, pp.1895–1914.
- Bian, J., Huo, R., Zhong, Y. and Guo, Z. (2024) 'XGB-Northern Goshawk optimization: predicting the compressive strength of self-compacting concrete', *KSCE Journal of Civil Engineering*, Vol. 28, No. 4, pp.1423–1439.
- Broomhead, D.S. and Lowe, D. (1988) *Radial Basis Functions, Multi-Variable Functional Interpolation, and Adaptive Networks*, No. RSREMEMO-4148, pp.1–34, Royal Signals and Radar Establishment Malvern, UK.
- Buhmann, M.D. (2000) 'Radial basis functions', *Acta Numerica*, Vol. 9, No. 1, pp.1–38.

- Cheng, M-Y., Prayogo, D. and Wu, Y-W. (2014) 'Novel genetic algorithm-based evolutionary support vector machine for optimizing high-performance concrete mixture', *Journal of Computing in Civil Engineering*, Vol. 28, No. 4, p.06014003.
- Chou, J-S. and Pham, A-D. (2013) 'Enhanced artificial intelligence for ensemble approach to predicting high performance concrete compressive strength', *Construction and Building Materials*, Vol. 49, pp.554–563.
- Chou, J-S., Chiu, C-K., Farfoura, M. and Al-Taharwa, I. (2011) 'Optimizing the prediction accuracy of concrete compressive strength based on a comparison of data-mining techniques', *Journal of Computing in Civil Engineering*, Vol. 25, No. 3, pp.242–253.
- Dao, D. Van, Adeli, H., Ly, H-B., Le, L.M., Le, V.M., Le, T-T. and Pham, B.T. (2020) 'A sensitivity and robustness analysis of GPR and ANN for high-performance concrete compressive strength prediction using a Monte Carlo simulation', *Sustainability*, Vol. 12, No. 3, p.830.
- Ding, M., Yu, R., Feng, Y., Wang, S., Zhou, F., Shui, Z., Gao, X., He, Y. and Chen, L. (2021) 'Possibility and advantages of producing an ultra-high performance concrete (UHPC) with ultra-low cement content', *Construction and Building Materials*, Vol. 273, p.122023.
- Elaiyaraja, P. and Boinapalli, N.R. (2024) 'Enhanced ferroelectric and piezoelectric properties in  $\text{NaNbO}_3$ -based materials via  $\text{BiGd/YKZrTiO}_3$  two-step sintering', *FMDb Transactions on Sustainable Applied Sciences*, Vol. 1, No. 1, pp.10–20.
- Erdal, H.I., Karakurt, O. and Namli, E. (2013) 'High performance concrete compressive strength forecasting using ensemble models based on discrete wavelet transform', *Engineering Applications of Artificial Intelligence*, Vol. 26, No. 4, pp.1246–1254.
- Esmacili-Falak, M. and Benemaran, R.S. (2024a) 'Application of optimization-based regression analysis for evaluation of frost durability of recycled aggregate concrete', *Structural Concrete*, Vol. 25, No. 1, pp.716–737.
- Esmacili-Falak, M. and Benemaran, R.S. (2024b) 'Ensemble extreme gradient boosting based models to predict the bearing capacity of micropile group', *Applied Ocean Research*, Vol. 151, No. 10, p.104149.
- Gandomi, A.H. and Alavi, A.H. (2012) 'A new multi-gene genetic programming approach to nonlinear system modeling. Part I: materials and structural engineering problems', *Neural Computing and Applications*, Vol. 21, No. 8, pp.171–187.
- Golafshani, E.M., Arashpour, M. and Behnood, A. (2022) 'Predicting the compressive strength of green concretes using Harris hawks optimization-based data-driven methods', *Construction and Building Materials*, Vol. 318, No. 2, p.125944.
- Gupta, M., Upreti, K., Yadav, S., Verma, M., Mageswari, M. and Tiwari, A. (2024) 'Assessment of ML techniques and suitability to predict the compressive strength of high-performance concrete (HPC)', *Asian Journal of Civil Engineering*, Vol. 25, No. 8, pp.5741–5752.
- Hadji, T., Guettala, S. and Quéneudec, M. (2021) 'Mix design of high performance concrete with different mineral additions', *World Journal of Engineering*, Vol. 18, No. 5, pp.767–779.
- Hir, M.A., Zaheri, M. and Rahimzadeh, N. (2023) 'Prediction of rural travel demand by spatial regression and artificial neural network methods (Tabriz County)', *Journal of Transportation Research (Tehran)*, Vol. 20, No. 4, pp.367–386.
- Hu, X. (2023) 'Use an adaptive network fuzzy inference system model for estimating the compressive strength of high-performance concrete with two optimizers improved grey wolf algorithm and dragonfly optimization algorithm', *Multiscale and Multidisciplinary Modeling, Experiments and Design*, Vol. 6, No. 2, pp.263–276.
- Ikwuagwu, C.V., Achebe, C.N. and Ononiwu, N.H. (2024a) 'Investigating variability in power capacity through experimental testing of lithium-ion batteries', *FMDb Transactions on Sustainable Energy Sequence*, Vol. 2, No. 1, pp.12–20.
- Ikwuagwu, C.V., Iroegbu, C.C., Onodu, J.C. and Okoh, I.E. (2024b) 'Comparative simulation studies on fabrication of thermos flask using glass fibre reinforced plastics and stainless steel', *FMDb Transactions on Sustainable Energy Sequence*, Vol. 2, No. 1, pp.21–32.



- Ikwuagwu, C.V., Ononiwu, N.H. and Adeyemi, K. (2023) 'Comprehensive energy analysis and performance evaluation of lithium-ion battery integration in photovoltaic systems: a comparative study on reliability and environmental impact', *FMDB Transactions on Sustainable Energy Sequence*, Vol. 1, No. 2, pp.83–93.
- Imran, M., Raza, A. and Touqeer, M. (2024) 'Prediction of compressive strength of high-performance concrete (HPC) using machine learning algorithms', *Multiscale and Multidisciplinary Modeling, Experiments and Design*, Vol. 7, No. 3, pp.1881–1894.
- Jasper, K.D., Jaishnav, M.N., Chowdhury, M.F., Badhan, R. and Sivakani, R. (2024) 'Defend and secure: a strategic and implementation framework for robust data breach prevention', *AVE Trends in Intelligent Computing Systems*, Vol. 1, No. 1, pp.17–31.
- Ji, T., Lin, T. and Lin, X. (2006) 'A concrete mix proportion design algorithm based on artificial neural networks', *Cement and Concrete Research*, Vol. 36, No. 7, pp.1399–1408.
- Kadam, S.S. and Deming, C. (2024) 'Reforming solar efficiency with a ground-breaking journey through advanced material innovations for high-performance photovoltaics', *FMDB Transactions on Sustainable Applied Sciences*, Vol. 1, No. 1, pp.44–53.
- Kadhim, K.H. and Lukutin, B. (2019) 'Mathematical modeling of solar heating system for an aluminum factory', *Journal of Advanced Research in Dynamical and Control Systems*, Vol. 11, No. 11, pp.198–205.
- Kadhim, K.H. and Lukutin, B. (2021) 'A study on solar thermal technologies and resources with an emphasis on solar power in Iraq', *Journal of Green Engineering*, Vol. 11, No. 2, pp.1811–1875.
- Kasperkiewicz, J., Racz, J. and Dubrawski, A. (1995) 'HPC strength prediction using artificial neural network', *Journal of Computing in Civil Engineering*, Vol. 9, No. 4, pp.279–284.
- Khan, M.I. and Abbas, Y.M. (2023) 'Robust extreme gradient boosting regression model for compressive strength prediction of blast furnace slag and fly ash concrete', *Materials Today Communications*, Vol. 35, No. 6, p.105793.
- Khorsheed, M.S. and Al-Thubaity, A.O. (2013) 'Comparative evaluation of text classification techniques using a large, diverse Arabic dataset', *Language Resources and Evaluation*, Vol. 47, No. 3, pp.513–538.
- Kisi, O. (2008) 'The potential of different ANN techniques in evapotranspiration modelling', *Hydrological Processes: An International Journal*, Vol. 22, No. 14, pp.2449–2460.
- Kisi, O. and Cigizoglu, H.K. (2007) 'Comparison of different ANN techniques in river flow prediction', *Civil Engineering and Environmental Systems*, Vol. 24, No. 3, pp.211–231.
- Kumar, C.S., Sathya, A., Deb, R. and Rahman, M.M. (2024) 'Managing electronic waste: a comprehensive review of current state and challenges', *FMDB Transactions on Sustainable Environmental Sciences*, Vol. 1, No. 1, pp.10–18.
- Lee, S., Nguyen, N., Karamanli, A., Lee, J. and Vo, T.P. (2023) 'Super learner machine-learning algorithms for compressive strength prediction of high performance concrete', *Structural Concrete*, Vol. 24, No. 2, pp.2208–2228.
- Lee, S-C. (2003) 'Prediction of concrete strength using artificial neural networks', *Engineering Structures*, Vol. 25, No. 7, pp.849–857.
- Leema, N., Nehemiah, H.K. and Kannan, A. (2016) 'Neural network classifier optimization using differential evolution with global information and back propagation algorithm for clinical datasets', *Applied Soft Computing*, Vol. 49, No. 12, pp.834–844.
- Li, E., Zhou, J., Shi, X., Armaghani, D.J., Yu, Z., Chen, X. and Huang, P. (2021) 'Developing a hybrid model of salp swarm algorithm-based support vector machine to predict the strength of fiber-reinforced cemented paste backfill', *Engineering with Computers*, Vol. 37, No. 3, pp.3519–3540.
- Li, W., Wang, R., Ai, Q., Liu, Q. and Lu, S.X. (2023) 'Estimation of compressive strength and slump of HPC concrete using neural network coupling with metaheuristic algorithms', *Journal of Intelligent & Fuzzy Systems*, Vol. 45, No. 1, pp.577–591.

- Lukutin, B. and Kadhim, K.H. (2021a) 'Application of a genetic algorithm for planning loads of a power supply system with a network photo-power plant and a heat active consumer', *Periodicals of Engineering and Natural Sciences*, Vol. 9, No. 4, pp.898–912.
- Lukutin, B.V. and Kadhim, K.H. (2021b) 'Photovoltaic power plants with electrochemical and thermal energy storage in Iraq', *Bulletin of the Tomsk Polytechnic University, Geo Assets Engineering*, Vol. 332, No. 1, pp.174–183.
- Lukutin, B.V., Shandarova, E.B. and Kadhim, K.H. (2022) 'Energy efficient algorithm for controlling photovoltaic power plant with electrochemical and thermal energy storage', *Bulletin of the Tomsk Polytechnic University, Geo Assets Engineering*, Vol. 333, No. 10, pp.22–30.
- Lyu, F., Fan, X., Ding, F. and Chen, Z. (2021) 'Prediction of the axial compressive strength of circular concrete-filled steel tube columns using sine cosine algorithm-support vector regression', *Composite Structures*, Vol. 273, No. 10, p.114282.
- Maraju, P.K. (2024) 'Advancing synergy of computing and artificial intelligence with innovations challenges and future prospects', *FMDB Transactions on Sustainable Intelligent Networks*, Vol. 1, No. 1, pp.1–14.
- Mathew, I.O., Otaraku, I., Oji, A. and Ikenyiri, P.N. (2024a) 'Addressing methane venting: strategies and implications on the environment', *FMDB Transactions on Sustainable Environmental Sciences*, Vol. 1, No. 1, pp.41–56.
- Mathew, I.O., Otaraku, I.J., Kareem, S.A., Oji, A. and Ikenyiri, P.N. (2024b) 'Delignification of different lignocellulosic biomass using hydrogen peroxide and acetic acid (HPAC)', *FMDB Transactions on Sustainable Environmental Sciences*, Vol. 1, No. 1, pp.19–30.
- Mehta, G., Bose, S.R. and Naveen, R.S. (2023) 'Optimizing lithium-ion battery controller design for electric vehicles: a comprehensive study', *FMDB Transactions on Sustainable Energy Sequence*, Vol. 1, No. 2, pp.60–70.
- Moodi, Y., Ghasemi, M. and Mousavi, S.R. (2022) 'Estimating the compressive strength of rectangular fiber reinforced polymer-confined columns using multi-layer perceptron, radial basis function, and support vector regression methods', *Journal of Reinforced Plastics and Composites*, Vol. 41, Nos. 3–4, pp.130–146.
- Mousavi, S.M., Aminian, P., Gandomi, A.H., Alavi, A.H. and Bolandi, H. (2012) 'A new predictive model for compressive strength of HPC using gene expression programming', *Advances in Engineering Software*, Vol. 45, No. 1, pp.105–114.
- Mudunuri, L.N.R. (2024) 'Artificial intelligence (AI) powered matchmaker: finding your ideal vendor every time', *FMDB Transactions on Sustainable Intelligent Networks*, Vol. 1, No. 1, pp.27–39.
- Nanban, D., Selvan, J., Christus, A.T.A. and Amin, M.A. (2024) 'Enhancing air traffic management: the transformative role of artificial intelligence in modern air traffic control', *FMDB Transactions on Sustainable Intelligent Networks*, Vol. 1, No. 2, pp.72–84.
- Nguyen, N-H., Vo, T.P., Lee, S. and Asteris, P.G. (2021) 'Heuristic algorithm-based semi-empirical formulas for estimating the compressive strength of the normal and high performance concrete', *Construction and Building Materials*, Vol. 304, No. 10, p.124467.
- Nguyen, T., Kashani, A., Ngo, T. and Bordas, S. (2019) 'Deep neural network with high-order neuron for the prediction of foamed concrete strength', *Computer-Aided Civil and Infrastructure Engineering*, Vol. 34, No. 4, pp.316–332.
- Nguyen, T-A. and Ly, H-B. (2024) 'Predicting axial compression capacity of CFDST columns and design optimization using advanced machine learning techniques', *Structures*, Vol. 59, No. 1, p.105724.
- Nwabuokei, I., Ghouse, M., Chen, W., Kollannur, E.T., Li, H. and Bin Sulaiman, R. (2023) 'Quantifying the influence of population on carbon emissions: a comparative study of developed versus developing countries using machine learning', *FMDB Transactions on Sustainable Energy Sequence*, Vol. 1, No. 2, pp.71–82.

- Nwezeh, E.N. (2023) 'The effect of water cement ratio and aggregatecement ratio on the 28 days strength of normal concrete', *Nau Department of Civil Engineering Final Year Project & Postgraduate Portal*, Vol. 2, No. 1, pp.1–66.
- Pandey, P., Lawanya, T. and Hasan, S.M.S. (2024) 'Heat transfer analysis of a stretching sheet in TRI particle-enhanced nanofluid systems', *FMDB Transactions on Sustainable Applied Sciences*, Vol. 1, No. 1, pp.21–33.
- Panyaram, S. (2024) 'Integrating artificial intelligence with big data for real-time insights and decision-making in complex systems', *FMDB Transactions on Sustainable Intelligent Networks*, Vol. 1, No. 2, pp.85–95.
- Pierini, J.O., Gómez, E.A. and Telesca, L. (2012) 'Prediction of water flows in Colorado River, Argentina', *Latin American Journal of Aquatic Research*, Vol. 40, No. 4, pp.872–880.
- Pierre, T.J., Rahman, M.M., Amin, M.A. and Munshi, M. (2024a) 'Deciphering urban footprints on climate variability through an innovative inquiry into heat island phenomena', *FMDB Transactions on Sustainable Applied Sciences*, Vol. 1, No. 1, pp.34–43.
- Pierre, T.J., Tao, C., Vénant, K. and Erneste, B. (2024b) 'Speed management blueprint: conception of an IoT-based electric vehicle speed limiter monitoring system for Kigali city vehicles', *FMDB Transactions on Sustainable Energy Sequence*, Vol. 2, No. 1, pp.33–48.
- Piro, N.S., Mohammed, A.S. and Hamad, S.M. (2022a) 'The impact of GGBS and ferrous on the flow of electrical current and compressive strength of concrete', *Construction and Building Materials*, Vol. 349, No. 9, p.128639.
- Piro, N.S., Mohammed, A.S., Hamad, S.M. and Kurda, R. (2022b) 'Electrical conductivity, microstructures, chemical compositions, and systematic multivariable models to evaluate the effect of waste slag smelting (pyrometallurgical) on the compressive strength of concrete', *Environmental Science and Pollution Research*, Vol. 29, No. 45, pp.68488–68521.
- Prakash, S., Kumar, S. and Rai, B. (2024) 'A new technique based on the gorilla troop optimization coupled with artificial neural network for predicting the compressive strength of ultrahigh performance concrete', *Asian Journal of Civil Engineering*, Vol. 25, No. 1, pp.923–938.
- Prasad, B.K.R., Eskandari, H. and Reddy, B.V.V. (2009) 'Prediction of compressive strength of SCC and HPC with high volume fly ash using ANN', *Construction and Building Materials*, Vol. 23, No. 1, pp.117–128.
- Pulivarthy, P. (2024) 'Semiconductor industry innovations: database management in the era of wafer manufacturing', *FMDB Transactions on Sustainable Intelligent Networks*, Vol. 1, No. 1, pp.15–26.
- Rafiei, M.H., Khushefati, W.H., Demirboga, R. and Adeli, H. (2017a) 'Novel approach for concrete mixture design using neural dynamics model and virtual lab concept', *ACI Materials Journal*, Vol. 114, No. 1, p.11.
- Rafiei, M.H., Khushefati, W.H., Demirboga, R. and Adeli, H. (2017b) 'Supervised deep restricted Boltzmann machine for estimation of concrete', *ACI Materials Journal*, Vol. 114, No. 2, p.237.
- Raja, A.S.V., Jasper, K.D., Poornima, V., Priscila, S.S., Thenmozhi, A. and Ratkovic, N. (2024) 'Tech horizons unveiled: navigating the transformative decade in AIML, cybersecurity, IoT, gaming, and data science education', *FMDB Transactions on Sustainable Intelligent Networks*, Vol. 1, No. 2, pp.120–134.
- Rajasekaran, S. and Lavanya, S. (2007) 'Hybridization of genetic algorithm with immune system for optimization problems in structural engineering', *Structural and Multidisciplinary Optimization*, Vol. 34, No. 1, pp.415–429.
- Ramya, L.N., Bose, S.R., Naveen, R.S. and Chowdhury, R.I. (2023) 'Advanced solar charge controller: integrating MPPT technology and online data logging for efficient energy management', *FMDB Transactions on Sustainable Energy Sequence*, Vol. 1, No. 2, pp.107–120.

- Regin, R., Gaayathri, R.S., Paramasivan, P., Rajest, S.S. and Radwan, R. (2024) 'VehiWalnut: smart fuel management with real-time data and user interaction', *FMDB Transactions on Sustainable Intelligent Networks*, Vol. 1, No. 1, pp.56–71.
- Regin, R., Obaid, A.J., Alenezi, A., Gupta, A.K. and Kadhim, K.H. (2021) 'Node replacement based energy optimization using enhanced salp swarm algorithm (ES2A) in wireless sensor networks', *Journal of Engineering Science and Technology*, Vol. 16, No. 3, pp.2487–2501.
- Rincon, L.F., Moscoso, Y.M., Hamami, A.E.A., Matos, J.C. and Bastidas-Arteaga, E. (2024) 'Degradation models and maintenance strategies for reinforced concrete structures in coastal environments under climate change: a review', *Buildings*, Vol. 14, No. 3, p.562.
- Santoso, L.W., Singh, B., Rajest, S.S., Regin, R. and Kadhim, K.H. (2021) 'A genetic programming approach to binary classification problem', *EAI Endorsed Transactions on Energy Web*, Vol. 8, No. 31, pp.1–8.
- Saxena, R.R., Saxena, R. and Patel, A. (2023) 'Functional electrical stimulation as a significant bioelectronic intervention in the domain of fitness: a review', *FMDB Transactions on Sustainable Energy Sequence*, Vol. 1, No. 2, pp.94–106.
- Sucharda, O., Gandel, R., Cmiel, P., Jerabek, J. and Bilek, V. (2024) 'Utilization of high-performance concrete mixtures for advanced manufacturing technologies', *Buildings*, Vol. 14, No. 8, p.2269.
- Suraj, D., Sulthan, N., Balaji, R., Swathi, R., Roberts, C. and Vaidianathan, B. (2024) 'Data-driven and domain adaptation framework for optimizing energy usage forecasting in smart buildings using ARIMA model', *FMDB Transactions on Sustainable Energy Sequence*, Vol. 2, No. 1, pp.1–11.
- Szolomicki, J. and Golasz-Szolomicka, H. (2019) 'Technological advances and trends in modern high-rise buildings', *Buildings*, Vol. 9, No. 9, p.193.
- Thirunagalingam, A. (2024a) 'Bias detection and mitigation in data pipelines: ensuring fairness and accuracy in machine learning', *AVE Trends in Intelligent Computing Systems*, Vol. 1, No. 2, pp.116–127.
- Thirunagalingam, A. (2024b) 'Transforming real-time data processing: the impact of AutoML on dynamic data pipelines', *FMDB Transactions on Sustainable Intelligent Networks*, Vol. 1, No. 2, pp.110–119.
- Tin, H.H.K., Thu, S. and Maung, K.K. (2024) 'A systematic review of rice husk gasifiers: technology, performance, and sustainability', *FMDB Transactions on Sustainable Environmental Sciences*, Vol. 1, No. 1, pp.31–40.
- Tiza, M.T., Imoni, S., Akande, E.O., Mogbo, O., Jiya, V.H. and Onuzulike, C. (2024) 'Revolutionizing infrastructure development: exploring cutting-edge advances in civil engineering materials', *Recent Progress in Materials*, Vol. 6, No. 3, pp.1–68.
- Usman, M. and Ullah, A. (2024) 'Blockchain technology implementation in libraries: an overview of potential benefits and challenges', *AVE Trends in Intelligent Computing Systems*, Vol. 1, No. 1, pp.42–53.
- Wang, L., Cao, Q., Zhang, Z., Mirjalili, S. and Zhao, W. (2022) 'Artificial rabbits optimization: a new bio-inspired meta-heuristic algorithm for solving engineering optimization problems', *Engineering Applications of Artificial Intelligence*, Vol. 114, No. 9, p.105082.
- Yan, K. and Shi, C. (2010) 'Prediction of elastic modulus of normal and high strength concrete by support vector machine', *Construction and Building Materials*, Vol. 24, No. 8, pp.1479–1485.
- Yeh, I-C. (1998a) 'Modeling concrete strength with augment-neuron networks', *Journal of Materials in Civil Engineering*, Vol. 10, No. 4, pp.263–268.
- Yeh, I-C. (1998b) 'Modeling of strength of high-performance concrete using artificial neural networks', *Cement and Concrete Research*, Vol. 28, No. 12, pp.1797–1808.
- Yeh, I-C. (1999) 'Design of high-performance concrete mixture using neural networks and nonlinear programming', *Journal of Computing in Civil Engineering*, Vol. 13, No. 1, pp.36–42.

- Yeh, I-C. (2003) ‘Prediction of strength of fly ash and slag concrete by the use of artificial neural networks’, *J. Chin. Inst. Civil Hydraul. Eng.*, Vol. 15, No. 4, pp.659–663.
- Yeh, I-C. (2006) ‘Analysis of strength of concrete using design of experiments and neural networks’, *Journal of Materials in Civil Engineering*, Vol. 18, No. 4, pp.597–604.
- Yeh, I-C. (2007) ‘Modeling slump flow of concrete using second-order regressions and artificial neural networks’, *Cement and Concrete Composites*, Vol. 29, No. 6, pp.474–480.
- Zain, M.F.M. and Abd, S.M. (2009) ‘Multiple regression model for compressive strength prediction of high performance concrete’, *Journal of Applied Sciences*, Vol. 9, No. 1, pp.155–160.
- Zaji, A.H. and Bonakdari, H. (2014) ‘Performance evaluation of two different neural network and particle swarm optimization methods for prediction of discharge capacity of modified triangular side weirs’, *Flow Measurement and Instrumentation*, Vol. 40, pp.149–156.
- Zanardo, E. (2024) ‘Chronostamp: a general-purpose run-time for data-flow computing in a distributed environment’, *AVE Trends in Intelligent Computing Systems*, Vol. 1, No. 2, pp.106–115.
- Zhang, S., Liu, C., Wang, W. and Chang, B. (2020) ‘Twin least square support vector regression model based on gauss-laplace mixed noise feature with its application in wind speed prediction’, *Entropy*, Vol. 22, No. 10, p.1102.
- Zhao, J., Sufian, M., Abuhussain, M.A., Althoey, F. and Deifalla, A.F. (2024) ‘Exploring the potential of agricultural waste as an additive in ultra-high-performance concrete for sustainable construction: a comprehensive review’, *Reviews on Advanced Materials Science*, Vol. 63, No. 1, p.20230181.